JOURNAL OF MATERIALS SCIENCE 29 (1994) 999–1003

CO_2 decomposition with mangano-wüstite

M. TABATA, H. KATO, T. KODAMA, T. YOSHIDA, M. TSUJI, Y. TAMAURA
Department of Chemistry, Research Centre for Carbon Recycling and Utilization, Tokyo Institute of Technology, Ookayama, Meguro-ku, Tokyo 152, Japan

Mn(II)-ferrite ($Mn_{0.97}Fe_{2.02}O_{4.00}$) prepared by the wet method was reduced in a hydrogen at 300 °C to form highly reactive mangano-wüstite (($Fe_{0.67}$, $Mn_{0.32}$)O) for CO_2 decomposition. Approximately 23% CO_2 injected (3.40 mmol) was decomposed to CO by the mangano-wüstite (3.22 g) in the initial stage of the reaction in a batch system at 400 °C. 88% CO was further decomposed to carbon. Approximately 58% CO_2 injected was reversibly adsorbed on the surface and the remaining 12% was unchanged after 200 h reaction. The mangano-wüstite was concurrently transformed to Mn(II)-bearing ferrite ($Mn_{0.23}Fe_{2.77}O_{4.00}$) and manganese-rich mangano-wüstite (($Fe_{0.60}$, $Mn_{0.40}$)O). The higher CO_2 decomposition capacity for this mangano-wüstite than that for oxygen-deficient Mn(II)-ferrite is discussed in detail, based on electron hopping and movement of ions in the bulk.

1. Introduction

The chemical transformation of CO_2 has been extensively investigated using electrochemical and photocatalytic methods [1–9], and catalytic reaction methods with metals or metal oxides [10–16]. The electrochemical and photocatalytic reactions provide CO or hydrocarbons, but do not allow decomposition of CO_2 to carbon. Some metals, such as barium, calcium, strontium, aluminium, copper and magnesium are known to decompose a small portion of CO_2 to carbon, in which reaction oxygen from CO_2 is incorporated into the metal [15, 16]. However, there has been no report of CO_2 decomposition to carbon by metal oxide in the absence of hydrogen gas. Recently, we reported the complete decomposition of CO_2 to carbon with oxygen-deficient magnetite ($Fe_3O_{4-\delta}$, δ = oxygen deficiency) at low temperature (300 °C) [17]. In this reaction, oxygen from CO_2 was incorporated on the oxygen-deficient site of the oxygen-deficient magnetite. The reaction rate and the capacity for CO_2 decomposition were enhanced when δ became large.

More recently, the CO_2 decomposition to carbon has been reported for oxygen-deficient Mn(II)-bearing ferrite ($Mn_xFe_{3-x}O_{4-\delta}$, $0 \leq x \leq 1$) at 300 °C [18, 19]. Increase in the manganese content of the compound lowered the CO_2 decomposition rate and capacity. The reaction rate and the capacity also varied with δ.

Baerns and co-workers [20–22] prepared mixed oxides of iron and manganese by calcination of mixed hydroxide precipitates of Fe(III) and Mn(II) ions at 120–500 °C. These oxides were reduced with hydrogen at 300–450 °C and the reduced materials were studied using the Fischer–Tropsch process

$$CO + H_2 \rightarrow \text{hydrocarbons} \qquad (1)$$

at 225–270 °C. However, their materials were mixtures of metallic iron, mangano-wüstite, Mn(II)-bearing ferrite and/or MnO. The proportion of each compound was dependent on the mole ratio of Mn/Fe in the mixed hydroxide precipitates. Their use of mixed material may be ascribed to their failure to synthesize a single-phase material. The use of the mixed material has complicated understanding of the process, although mangano-wüstite phase may have played a central part in the chemical conversion.

Mangano-wüstite is a solid solution of wüstite (Fe_yO, $y < 1$) and manganese(II) oxide (Mn_zO, $z < 1$) with the NaCl structure. Oxygen ions are cubic close packed in both mangano-wüstite and oxygen-deficient Mn(II)-ferrite. Hence, the mangano-wüstite with the chemical composition ($Fe_{0.66}$, $Mn_{0.33}$)O can be regarded as an oxygen-deficient Mn(II)-ferrite with $\delta = 1$. Therefore, it can be expected that the mangano-wüstite will have a degree of CO_2 decomposition reactivity at ~ 300 °C. The objectives of this research were to synthesize single-phase mangano-wüstite and to understand its CO_2 decomposition reactivity in comparison with oxygen-deficient Mn(II)-ferrite.

2. Experimental Procedure

2.1. Materials

All the chemicals used were of analytical grade, and distilled water was used for the preparation of the solution. $FeSO_4 \cdot 7H_2O$, $MnSO_4 \cdot 4\text{–}6H_2O$ and NaOH were supplied by Wako Chemical Industries Ltd.

2.2. Preparation of Mn(II)-ferrite and mangano-wüstite

Mn(II)-ferrite was synthesized by air oxidation of an aqueous suspension according to the method reported previously [18, 23]. It is briefly described as follows: any dissolved oxygen gas in distilled water

(4.0 dm^3) was removed by passing nitrogen gas through for a few hours and $FeSO_4 \cdot 7H_2O$ (300 g) and $MnSO_4 \cdot 4\text{–}6H_2O$ (127 g) were added to prepare the mixed solution. The pH of the solution was raised to 10 by adding 3 mol dm^{-3} NaOH solution to form a mixed hydroxide. The suspension was air-oxidized by bubbling air for 5 h at 65 °C while the pH was kept constant at 10 by adding NaOH solution. The product was collected by decantation. After successive washing with distilled water and acetone, the product was dried in a nitrogen gas stream at room temperature.

Single-phase mangano-wüstite was prepared as follows: Mn(II)-ferrite was reduced by passing hydrogen gas at a flow rate of 50×10^{-3} dm^3 min^{-1} through a quartz reaction cell (24 mm diameter and 250 mm long) for 17 h at 300 °C. The sample was then quenched into a refrigerant of ice and stored in a nitrogen atmosphere. X-ray diffractometry with FeK_α radiation (Rigaku model RAD-2A diffractometer) was carried out with the reduced sample covered by polyethylene film in order to prevent oxidation. The infrared spectra of the products were measured by the KBr technique (Shimadzu model FTIR-8000). The chemical composition of the product was determined by colorimetry (Hitachi spectrophotometer model 124) using the 2,2′-bypyridine method [24, 25] for the mole ratio of Fe^{2+} to Fe_{total}, and by atomic absorption spectroscopy (Varian Techtron model AA-875) for the mole ratio of manganese to iron.

2.3. CO_2 decomposition reactivity of mangano-wüstite

CO_2 decomposition with mangano-wüstite was performed in a quartz cell. The equipment was as previously reported [18]. The experimental procedure was nearly the same as that of the previous paper and is briefly described as follows: mangano-wüstite obtained by reduction of 4.00 g Mn(II)-ferrite was heated in a quartz cell at 300 °C for 10 min in flowing nitrogen gas. Then, the reaction cell was evacuated, followed by CO_2 gas injection up to a pressure of 1.013×10^5 Pa. All the valves of the reaction cell were then closed (recorded as zero reaction time) and the internal pressure was measured with a pressure gauge. The internal gas contents were determined by gas chromatography (Shimadzu model GC-8A). The solid sample after reaction was quenched by quickly placing the reaction cell into a refrigerant of ice and identified by X-ray diffractometry with FeK_α radiation. For determination of the amount of deposited carbon, the reacted sample was dissolved in concentrated hydrochloric acid (~ 12 mol dm^{-3}). The black residue was percolated on a lump of quartz wool and determined for collected carbon using an elemental analyser (Perkin–Elmer model 2400 CHN).

3. Results and discussion

3.1. Characterization of Mn(II)-ferrite and mangano-wüstite

The X-ray diffraction (XRD) pattern of the prepared Mn(II)-ferrite showed only peaks corresponding to those of a spinel-type compound (Fig. 1a). The lattice constant evaluated according to the extrapolation function (Nelson–Riley function) was 0.8498 nm, which was equal to that reported in the JCPDS card for stoichiometric Mn(II)-ferrite (0.8499 nm) [26]. The infrared spectra of the products showed no peaks assigned to by-products of iron and/or manganese oxide hydroxides. The chemical analysis also showed that the Mn(II)-ferrite had a nearly stoichiometric chemical composition ($Mn_{0.97}Fe_{2.02}O_{4.00}$).

Reduction of the Mn(II)-ferrite for 8–10 h was insufficient for obtaining single-phase mangano-wüstite. The XRD pattern of the Mn(II)-ferrite reduced for 19 h showed peaks corresponding to α-Fe and mangano-wüstite phases. Therefore, the optimum reduction time for its preparation was 15–17 h. The XRD patterns of the hydrogen-reduced Mn(II)-ferrite for 17 h at 300 °C could be indexed by mangano-wüstite with the NaCl structure and showed no peaks of metallic iron or manganese, wüstite, MnO or Mn(II)-ferrite (Fig. 1b). The lattice constant, a_0, was 0.4368 nm, which was larger than that of wüstite (0.4307 nm) [27] and smaller than that of the stoichiometric MnO (0.4448 nm) [28]. The manganese content in the mangano-wüstite calculated from the relationship between the manganese content and the lattice constant reported by Foster and Welch [29] was 30 mol %. The manganese content of the

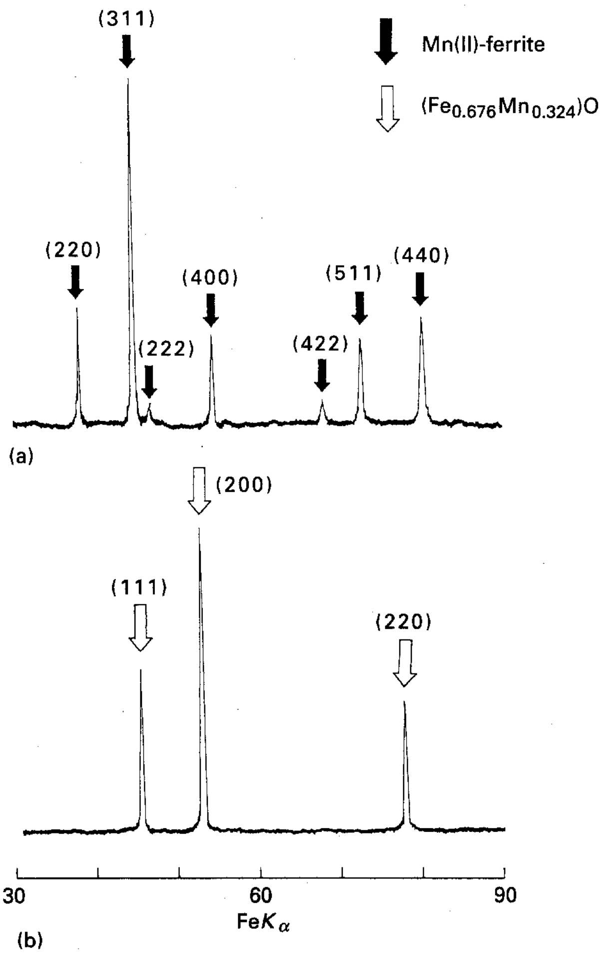

Figure 1 X-ray diffraction patterns of (a) Mn(II)-ferrite, and (b) mangano-wüstite, prepared by hydrogen reduction of Mn(II)-ferrite for 17 h at 300 °C.

mangano-wüstite (32 mol %) was in good agreement with the calculated value. Thus, single-phase mangano-wüstite could be synthesized by the hydrogen reduction of Mn(II)-ferrite at 300 °C.

3.2. CO_2 decomposition with mangano-wüstite

The variation with time of the gas contents of CO_2 and CO during the CO_2 decomposition with the mangano-wüstite at 300 °C were studied (Fig. 2a). The amount of CO_2 decreased drastically, accompanied by the evolution of CO. No other gases were observed during the reaction. The amount of evolved CO was nearly equal to that of the decreased CO_2 in the first 2 h of the reaction. CO decomposition to carbon did not proceed during this period. The partial pressures of CO_2 and CO appeared thereafter to be constant up to 45 h. A different feature was observed for in the variation with time of the gas contents of CO_2 and CO during the CO_2 decomposition reaction at 400 °C (Fig. 2b). The amount of CO_2 decreased from 100% to about 77% immediately after the injection of CO_2, and concurrently CO gas was evolved. The amount of CO was about 23% of the initial amount of CO_2, which was equal to the amount by which CO_2 diminished. The partial pressures of CO_2 and CO were still decreasing even after 45 h at 400 °C, and were therefore studied in further detail.

The mole ratio of CO_2 to CO decreased from 2.7:1 (after 5 h) to 2.0:1 (after 45 h) at 400 °C (Fig. 3). The amount of CO_2 gradually decreased to 18% of the initial CO_2 content after 200 h. The amount of remaining CO was 10% and the amount of carbon deposited was determined to be 20% of the introduced amount of CO_2. The apparent imbalance with respect to carbon can be attributed to the adsorption of CO_2 and/or CO on the surface.

In general, adsorption equilibrium is believed to be attained rapidly. For example, adsorption equilibration was reported to be attained within 100 min in a typical adsorption system on zeolite [30]. The adsorption on the mangano-wüstite is complicated due to simultaneous decomposition of CO_2 to CO and carbon, and concurrent phase transformation of the mangano-wüstite to Mn(II)-bearing ferrite, as will be described in Section 3. Owing to its association with the CO_2 decomposition reaction with mangano-wüstite, a small portion of the mangano-wüstite was transformed to Mn(II)-bearing ferrite, the amount of which was increased as the reaction proceeded. Mn(II)-bearing ferrite has been known to adsorb CO_2 on its surface [18, 19]; therefore, the reaction of CO_2 with the mangano-wüstite involves decomposition of CO_2 to CO and/or carbon, and adsorption of CO_2. Further studies are needed to estimate the contribution of each to the process.

3.3. Phase variation of mangano-wüstite during CO_2 decomposition reaction

The XRD pattern of the sample after 200 h reaction showed additional small diffraction peaks besides those of mangano-wüstite. They could be assigned to the spinel-type Mn(II)-bearing ferrite. This was formed by the incorporation of oxygen from the CO_2 molecule onto the crystal lattice of the NaCl structure of the mangano-wüstite.

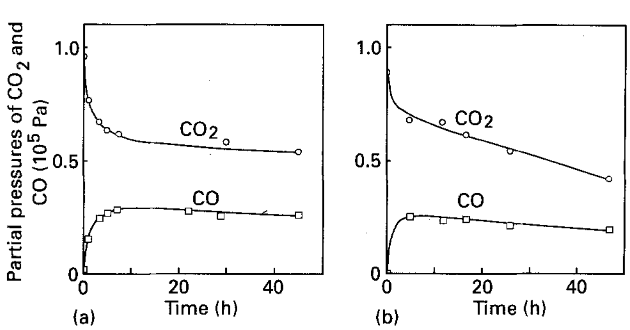

Figure 2 Change in the composition of CO_2 and CO in the reaction cell during the CO_2 decomposition reaction with mangano-wüstite as a function of reaction time at (a) 300 °C, and (b) 400 °C.

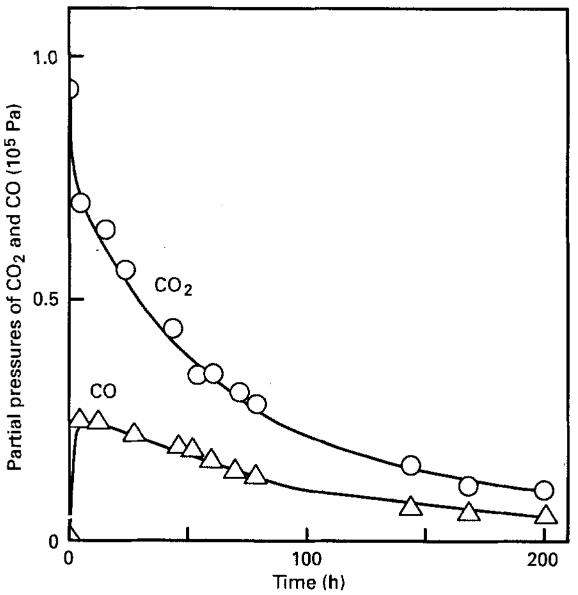

Figure 3 Change in the composition of CO_2 and CO in the reaction cell during the CO_2 decomposition reaction with mangano-wüstite as a function of reaction time at 400 °C.

TABLE I Change in the lattice constant, a_0, of mangano-wüstite and Mn(II)-bearing ferrite formed during CO_2 decomposition as a function of time

Reaction time (h)	Lattice constant (nm)	
	Mangano-wüstite	Mn(II)-bearing ferrite
0	0.4368	[a]
24	0.4370	[a]
48	0.4371	0.8422
96	0.4371	0.8422
144	0.4376	0.8422

[a] Mangano-wüstite phase only.

Table I summarizes the changes in the solid phase and the lattice constant during the CO_2 decomposition reaction. The lattice constant of the mangano-wüstite phase was increased from 0.4368 nm to 0.4376 nm as the reaction proceeded. It corresponds to the mangano-wüstite with 40 mol % MnO [29]. The lattice constant of the spinel phase was nearly constant during the reaction at 0.8422 nm, which corresponds to a Mn(II)-bearing ferrite with a composition of $Mn_{0.23}Fe_{2.77}O_{4.00}$ [31]. These findings led to the conclusion that the CO_2 decomposition to carbon was accompanied by simultaneous transformation of the mangano-wüstite (NaCl structure) into two phases of iron-rich Mn(II)-bearing ferrite (spinel structure) and Mn(II)-rich mangano-wüstite.

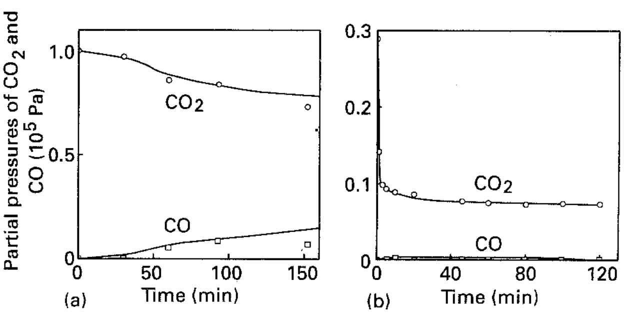

Figure 4 Change in the composition of CO_2 and CO in the reaction cell during the CO_2 decomposition reaction with (a) mangano-wüstite and (b) oxygen-deficient Mn(II)-ferrite, as a function of reaction time at 300 °C.

3.4. Comparison of CO_2 decomposition reactivity between mangano-wüstite and oxygen-deficient Mn(II)-ferrite

The variation with time in gas content were compared for the CO_2 decomposition with the mangano-wüstite and the oxygen-deficient Mn(II)-ferrite [18] at 300 °C (Fig. 4a and b). The reaction conditions for the CO_2 decomposition with the oxygen-deficient Mn(II)-ferrite were as follows: 2.00 g oxygen-deficient Mn(II)-ferrite ($Mn_{0.97}Fe_{2.03}O_{3.92}$) and 20×10^{-3} dm^3 CO_2. The reaction cell was 20 mm diameter and 200 mm long. The oxygen-deficient Mn(II)-ferrite was synthesized by hydrogen reduction (flow rate 0.20 $dm^3 min^{-1}$) for 20 min at 300 °C. The weight of the samples and the volume of CO_2 introduced were different from those for the mangano-wüstite. However, the volumes of CO_2 injected per weight were the same: 16.8×10^{-3} and 16.9×10^{-3} $dm^3 g^{-1}$ for the mangano-wüstite and the oxygen-deficient Mn(II)-ferrite, respectively. With the oxygen-deficient Mn(II)-ferrite (Fig. 4b), the amount of CO_2 rapidly decreased and became less than 50% in 10 min. Thereafter, the amount of CO_2 became nearly constant. A very small fraction of CO was evolved upon CO_2 injection. No other gases were observed during the reaction. The amount of deposited carbon was less than 0.7% of the injected amount of CO_2. The rapid decrease in the amount of CO_2 was ascribed mostly to the non-specific adsorption of CO_2 on the surface of the oxygen-deficient Mn(II)-ferrite. On the other hand, the decrease in the amount of CO_2 was not very rapid during the CO_2 decomposition reaction with the mangano-wüstite (Fig. 4a). The amount by which CO_2 decreased was nearly equal to that of evolved CO. This indicates that CO_2 was not simply adsorbed on the surface of the solid, but reduced to CO. Thus, the mangano-wüstite was found to have more reactive sites than the oxygen-deficient Mn(II)-ferrite with respect to the CO_2 reduction to CO.

The reason for this difference can be considered as follows: both the oxygen-deficient Mn(II)-ferrite and the mangano-wüstite are composed of cubic close packed oxygen ions in their crystal structure. A major difference between these oxides is the valence of the iron ions. The major cations are Mn^{2+} and Fe^{2+} in the mangano-wüstite, and Mn^{2+} and Fe^{3+} in the oxygen-deficient Mn(II)-ferrite. The population of Fe^{2+} ions is only 8% of the total iron ions in the latter material [18]. Mn^{2+} ions are not known to contribute to the CO_2 decomposition reaction [18, 19], only Fe^{2+} ions can donate electrons to the CO_2 on the solid surface and contribute to the CO_2 decomposition reaction. Thus, Fe^{2+} ions on the surface act as the reactive sites. Thus, the population density of the reactive sites in the mangano-wüstite is much larger than that in the oxygen-deficient Mn(II)-ferrite. The higher decomposition capacity of CO_2 to CO and/or carbon in the mangano-wüstite is due to the more abundant reactive sites in comparison with the oxygen-deficient Mn(II)-ferrite.

The phase transformations of the mangano-wüstite and the oxygen-deficient Mn(II)-ferrite during CO_2 decomposition reaction can be understood based on the movement of ions and electron hopping as follows: upon adsorption of CO_2 on the surface of these solids, oxygen ions are incorporated into the crystal face. Electrons of Fe^{2+} ions are donated to the CO_2 adsorbed on the surface, which causes the oxidation of Fe^{2+} to Fe^{3+} ions and movement of cations in the bulk toward the surface for electroneutrality. In the oxygen-deficient Mn(II)-ferrite, cations are subjected to redistribution by both migration of cations and electron hopping between the octahedral sites in the spinel structure. The movement of electrons from Fe^{2+} ions in the bulk based on the electron hopping causes redistribution of cations, forming Mn(II)-ferrite. In this process, Fe^{2+} ions in the octahedral sites play a central part. In the mangano-wüstite with the NaCl structure, electron hopping is not found between Fe^{2+} and Fe^{3+} ions in the octahedral site [32]. Hence, the distribution of ions is determined only by the movement of cations, because the mobility of cations is much larger than that of oxygen in the spinel structure [33, 34]. Therefore, the rate of the decomposition reaction with the mangano-wüstite was smaller than that with the oxygen-deficient Mn(II)-ferrite. The formation of two phases of the Mn(II)-bearing ferrite and the manganese-rich mangano-wüstite from single phase mangano-wüstite is due to the difference in the mobility of manganese and iron ions under the above conditions.

4. Conclusion

Single-phase mangano-wüstite and oxygen-deficient Mn(II)-ferrite have been studied; the former was prepared by hydrogen reduction of Mn(II)-ferrite ($Mn_{0.97}Fe_{2.02}O_{4.00}$) at 300 °C. The mangano-wüstite

($(Fe_{0.67}, Mn_{0.32})O$) exhibited a higher CO_2 decomposition capacity than the latter compound. The higher capacity can be attributed to a larger population density of reactive sites in the mangano-wüstite compared to that of the oxygen-deficient Mn(II)-ferrite. The mangano-wüstite was concurrently transformed to Mn(II)-bearing ferrite ($Mn_{0.23}Fe_{2.77}O_{4.00}$) and manganese-rich mangano-wüstite ($(Fe_{0.60}, Mn_{0.40})O$). The CO_2 decomposition process can be understood in relation to the movement of ions and electron hopping in the mangano-wüstite and the oxygen-deficient Mn(II)-ferrite.

References

1. J. C. HEMMINGER, R. CARR and G. A. SOMORJAI, *Chem. Phys. Lett.* **57** (1978) 100.
2. T. INOUE, A. FUJISHIMA, S. KONISHI and K. HONDA, *Nature (Lond.)* **277** (1979) 637.
3. Y. HORI, A. MURATA and R. TAKAHASHI, *J. Chem. Soc. Faraday Trans. I* **85** (1989) 2309.
4. J. HAWECKER, J. -M. LEHN and R. ZIESSEL, *Helv. Chem. Acta* **69** (1986) 1990.
5. B. A. PARKINSON and P. F. WEAVER, *Nature (Lond.)* **309** (1984) 148.
6. R. ZIESSEL, J. HAWECKER and J.-M. LEHN, *Helv. Chim. Acta* **69** (1986) 1065.
7. S. IKEDA, T. TAKAGI and K. ITO, *Bull. Chem. Soc. Jpn* **60** (1987) 2517.
8. I. WILLNER and D. MANDLER, *J. Am. Chem. Soc.* **111** (1989) 1330.
9. M. GRÄTZEL, A. J. McEVOY, K. R. TAMPI and C. REVILLIOD, in "Proceedings of International Symposium on Chemical Fixation of Carbon Dioxide", Nagoya, 1991, edited by K. Ito (Chemical Society of Japan, Research Group on Fixation of Carbon Dioxide, Nagoya, Japan, 1991) pp. 1–10.
10. K. OTSUKA, *Hyomen* **23** (1985) 206.
11. M. A. ULLA, R. A. MIGONE, J. O. PETUNCHI and E. A. LOMBARDO, *J. Catal.* **105** (1987) 107.
12. M.-D. LEE, J.-F. LEE and C.-S. CHANG, *J. Chem. Eng. Jpn* **23** (1990) 130.
13. R. C. WAGNER, R. CARRASQUILLO, J. EDWARDS and R. HOLMES, in "Proceedings of 18th Intersociety Conference on Environmental Systems", SAE Technical Paper Series 880995 (Society of Automotive Engineers, Warrendale, PA, 1988) pp. 1–9.
14. T. SUZUKI, K. SAEKI, Y. MAYAMA, T. HIRAI and S. HAYASHI, *React. Kinet. Catal. Lett.* **44** (1991) 489.
15. "*Gmelins Handbuch der Anorganischen Chemie*", 8th Edn, Kohlenstoff Part C2, edited by K. V. Baczko (Springer Verlag, Berlin, 1972) pp. 203.
16. R. G. COPPERTHWAITE, P. R. DAVIES, M. A. MORRIS, M. W. ROBERTS and R. A. RYDER, *Catal. Lett.* **1** (1988) 11.
17. Y. TAMAURA and M. TABATA, *Nature (Lond.)* **346** (1990) 255.
18. M. TABATA, Y. NISHIDA, T. KODAMA, K. MIMORI, T. YOSHIDA, and Y. TAMAURA, *J. Mater. Sci.* **28** (1993) 971.
19. M. TABATA, K. AKANUMA, K. NISHIZAWA, K. MIMORI, T. YOSHIDA, M. TSUJI and Y. TAMAURA, *ibid.*
20. N. K. JAGGI, L. H. SCHWARTZ, J. B. BUTT, H. PAPP and M. BAERNS, *Appl. Catal.* **13** (1985) 347.
21. G. C. MAITI, R. MALESSA, U. LÖCHNER, H. PAPP and M. BAERNS, *ibid.* **16** (1985) 215.
22. U. LÖCHNER, H. PAPP and M. BAERNS, *ibid.* **23** (1986) 339.
23. M. KIYAMA, *Bull. Chem. Soc. Jpn* **51** (1978) 134.
24. I. IWASAKI, T. KATSURA, T. OZAWA, M. YOSHIDA, M. MASHIMA, H. HARASHIMA and B. IWASAKI, *Bull. Volcanol. Soc. Jpn Ser. II* **5** (1960) 9.
25. J. T. WOODS and M. G. MELLON, *Ind. Eng. Chem. Anal. Ed.* **13** (1941) 551.
26. Powder Diffraction File, Card no. 10–319 (Joint Committee on Powder Diffraction Standard, Swarthmore, PA, 1967).
27. Powder Diffraction File, Card no. 6–615 (Joint Committee on Powder Diffraction Standard, Swarthmore, PA, 1967).
28. Powder Diffraction File, Card no. 7–230 (Joint Committee on Powder Diffraction Standard, Swarthmore, PA, 1967).
29. P. K. FOSTER and A. J. E. WELCH, *Trans. Faraday Soc.* **52** (1956) 1626.
30. R. P. TOWNSEND (ed.), "The Properties and Applications of Zeolites", Special Publications 33 (The Chemical Society, London, 1980).
31. Z. FUNATOGAWA, N. MIYATA and S. USAMI, *J. Phys. Soc. Jpn* **14** (1959) 1583.
32. C. GOHY, A. GERAND and F. GRANDJEAN, *Phys. Status Solidi. A* **74** (1982) 583.
33. R. LINDER and Å. ÅKERSTRÖM, *Z. Phys. Chem. N. F.* **18** (1956) 303.
34. K. ANDO and Y. OISHI, *J. Chem. Phys.* **61** (1974) 625.

Received 16 February
and accepted 4 June 1993